Modeling synchronization in networks of delay-coupled fiber ring lasers

Brandon S. Lindley and Ira B. Schwartz*

U.S. Naval Research Laboratory, Code6792, Plasma Physics Division, Nonlinear Systems Dynamics Section, Washington, D.C. 20375, USA

*ira.schwartz@nrl.navy.mil

Abstract: We study the onset of synchronization in a network of N delay-coupled stochastic fiber ring lasers with respect to various parameters when the coupling power is weak. In particular, for groups of three or more ring lasers mutually coupled to a central hub laser, we demonstrate a robust tendency toward out-of-phase (achronal) synchronization between the $N-1$ outer lasers and the single inner laser. In contrast to the achronal synchronization, we find the outer lasers synchronize with zero-lag (isochronal) with respect to each other, thus forming a set of $N-1$ coherent fiber lasers.

© 2011 Optical Society of America

OCIS codes: (190.4370) Nonlinear optics, fibers; (140.1540) Chaos; (140.3290) Laser arrays.

References and links

1. M. Mackey and L. Glass, "Oscillation and chaos in physiological control systems," Science **197**, 289–289 (1977).
2. M. Kim, M. Bertram, M. Pollmann, A. von Oertzen, A. S. Mikhailov, H. H. Rotermund, and G. Ertl, "Controlling chemical turbulence by global delayed feedback: pattern formation in catalytic co oxidation on pt(110)," Science **292**, 1357–1360 (2001).
3. K. Ikeda, "Multiple-valued stationary state and its instability of the transmitted light by a ring cavity system," Optics Commun. **30**, 257–261 (1979).
4. R. Lang and K. Kobayashi, "External optical feedback effects on semiconductor injection laser properties," IEEE J. Quantum Electron. **16**, 347–355 (1980).
5. D. V. R. Reddy, A. Sen, and G. L. Johnston, "Experimental evidence of time-delay-induced death in coupled limit-cycle oscillators," Phys. Rev. Lett. **85**, 3381–3384 (2000).
6. M. G. Rosenblum, A. S. Pikovsky, and J. Kurths, "Phase synchronization of chaotic oscillators," Phys. Rev. Lett. **76**, 1804–1807 (1996).
7. M. G. Rosenblum, A. S. Pikovsky, and J. Kurths, "From phase to lag synchronization in coupled chaotic oscillators," Phys. Rev. Lett. **78**, 4193–4196 (1997).
8. A. Wagemakers, J. M. Buldu, and M. Sanjuan, "Isochronous synchronization in mutually couple chaotic circuits," Chaos **17**, 023128 (2007).
9. O. D. Huys, R. Vicente, J. Danckaert, and I. Fischer, "Amplitude and phase effects on the synchronication of delay-couple oscillators," Chaos **20**, 043127 (2010).
10. J. Mulet, C. Mirasso, T. Heil, and I. Fischer, "Synchronication scenario of two distant mutually coupled semiconductor lasers," J. Opt. B: Quantum Semiclassical Opt. **6**, 97–105 (2004).
11. T. Heil, I. Fischer, W. Elsasser, J. Mulet, and C. R. Mirasso, "Chaos synchronization and spontaneous symmetry-breaking in symmetrically delay-coupled semiconductor lasers," Phys. Rev. Lett. **86**, 795–798 (2001).
12. J. K. White, M. Matus, and J. V. Moloney, "Achronal generalized synchronization in mutually coupled semiconductor lasers," Phys. Rev. E **65**, 036229 (2002).
13. Q. L. Williams and R. Roy, "Fast polarization dynamics of an erbium-doped fiber ring laser," Opt. Lett. **21**, 1478–1480 (1996).
14. Q. L. Williams, J. Garcia-Ojalvo, and R. Roy, "Fast intracavity polarization dynamics of an erbium-doped fiber ring laser: Inclusion of stochastic effects," Phys. Rev. A **55**, 2376–2386 (1997).
15. G. D. Vanwiggeren and R. Roy, "Chaotic communication using time-delayed optical systems," Int. J. Bifurcation Chaos Appl. Sci. Eng. **9**, 2129–2156 (1999).
16. R. Wang and K. Shen, "Synchronization of chaotic erbium-doped fiber dual-ring lasers by using the method of another chaotic system to drive them," Phys. Rev. E **65**, 016207 (2002).

#152747 - $15.00 USD Received 11 Aug 2011; revised 21 Oct 2011; accepted 24 Oct 2011; published 15 Nov 2011

Report Documentation Page

Form Approved
OMB No. 0704-0188

Public reporting burden for the collection of information is estimated to average 1 hour per response, including the time for reviewing instructions, searching existing data sources, gathering and maintaining the data needed, and completing and reviewing the collection of information. Send comments regarding this burden estimate or any other aspect of this collection of information, including suggestions for reducing this burden, to Washington Headquarters Services, Directorate for Information Operations and Reports, 1215 Jefferson Davis Highway, Suite 1204, Arlington VA 22202-4302. Respondents should be aware that notwithstanding any other provision of law, no person shall be subject to a penalty for failing to comply with a collection of information if it does not display a currently valid OMB control number.

1. REPORT DATE **15 NOV 2011**	2. REPORT TYPE	3. DATES COVERED **00-00-2011 to 00-00-2011**
4. TITLE AND SUBTITLE **Modeling Synchronization In Networks Of Delay-Coupled Fiber Ring Lasers**		5a. CONTRACT NUMBER
		5b. GRANT NUMBER
		5c. PROGRAM ELEMENT NUMBER
6. AUTHOR(S)		5d. PROJECT NUMBER
		5e. TASK NUMBER
		5f. WORK UNIT NUMBER
7. PERFORMING ORGANIZATION NAME(S) AND ADDRESS(ES) **U.S. Naval Research Laboratory,Code6792, Plasma Physics Division,Nonlinear Systems,Washington,DC,20375**		8. PERFORMING ORGANIZATION REPORT NUMBER
9. SPONSORING/MONITORING AGENCY NAME(S) AND ADDRESS(ES)		10. SPONSOR/MONITOR'S ACRONYM(S)
		11. SPONSOR/MONITOR'S REPORT NUMBER(S)
12. DISTRIBUTION/AVAILABILITY STATEMENT **Approved for public release; distribution unlimited**		
13. SUPPLEMENTARY NOTES **Opt. Express 19, 24460-24467 (2011), November 15, 2011**		
14. ABSTRACT		
15. SUBJECT TERMS		

16. SECURITY CLASSIFICATION OF:			17. LIMITATION OF ABSTRACT	18. NUMBER OF PAGES	19a. NAME OF RESPONSIBLE PERSON
a. REPORT **unclassified**	b. ABSTRACT **unclassified**	c. THIS PAGE **unclassified**	**Same as Report (SAR)**	**9**	

Standard Form 298 (Rev. 8-98)
Prescribed by ANSI Std Z39-18

17. Y. Imai, H. Murakawa, and T. Imoto, "Chaos synchronization characteristics in erbium-doped fiber laser systems," Opt. Commun. **217**, 415–420 (2003).
18. D. J. DeShazer, B. P. Tighe, M. Kurths, and R. Roy, "Experimental observation of noise-induced synchronization of bursting dynamical systems," IEEE J. Sel. Top. Quantum Electron. **10**, 906–910 (2004).
19. L. B. Shaw, I. B. Schwartz, E. A. Rogers, and R. Roy, "Synchronization and time shifts of dynamical patterns for mutually delay-coupled fiber ring lasers," Chaos **16**, 01511 (2006).
20. I. B. Schwartz and L. B. Shaw, "Isochronal synchronization of delay-coupled systems," Phys. Rev. E **75**, 046207 (2007).
21. A. L. Franz, R. Roy, L. B. Shaw, and I. B. Schwartz, "Changing dynamical complexity with time delay in coupled fiber laser oscillators," Phys. Rev. Lett. **99**, 053905 (2007).
22. C. Massoller and A. Marti, "Random delays and the sychronization of chaotic maps," Phys. Rev. Lett. **94**, 134102 (2005).
23. E. A. Rogers, "Synchronization of high dimensional dynamical systems," Ph.D. thesis, University of Maryland College Park (2005).
24. E. A. Rogers-Dakin, J. Garcia-Ojalvo, D. J. Deshazer, and R. Roy, "Synchronization and symmetry breaking in mutually coupled fiber lasers," Phys. Rev. E **73**, 045201 (2006).
25. A. S. Landsman and I. B. Schwartz, "Complete chaotic synchronization in mutually coupled time-delay systems," Phys. Rev. E **75**, 026201 (2007).
26. J. Zamora-Munt, C. Masoller, J. Garcia-Ojalvo, and R. Roy, "Crowd synchrony and quorum sensing in delay-coupled lasers," Phys. Rev. Lett. **105**, 264101 (2010).
27. D. Tsygankov and K. Wiesenfeld, "Weak link synchronization," Phys. Rev. E **73**, 026222 (2006).
28. L. Kocarev and U. Parlitz, "Generalized synchronization, predictability, and equivalence of unidirectionally coupled dynamical systems," Phys. Rev. Lett. **76**, 1816–1819 (1996).

1. Introduction

The dynamics of delay-coupled systems is a rich and varied area of study covering a wide range of topics from biological systems [1], to chemical reactions [2], to physical systems such as laser systems [3,4] and electrical circuits [5]. Understanding the behavior of such dynamical systems generally involves solving systems of delay differential equations, and these systems often exhibit chaotic behavior and other complicated phenomenon such as noise-induced oscillations. For example, delay-coupled nonlinear oscillators exhibit complex phenomena such as generalized, phase, and lag synchronization [6, 7] in the chaotic regimes.

Systems of delay-coupled oscillators often exhibit a time lag between individual nodes, with a leading time series followed by a lagging one. That is, lagged phase synchronization occurs when the time series are correlated but locked in phase at a value other than zero. Such lagged synchronization is called achronal synchronization, and has been studied for many delay-coupled dynamical oscillators, such as mutually coupled chaotic circuits [8], and Kuramoto and Stuart-Landau oscillators [9]. In particular, achronal synchronization is of special interest to those studying coupled arrays of nonlinear optical systems, such as semiconductor or fiber ring lasers [10]. This is due to the fact that in general coupled lasing systems, the synchronized state with zero-lag is unstable. Due to the injection of noise, the unstable achronal state may exhibit spontaneous switching between leading and lagging nodes [11].

There has been substantial progress in understanding delay-coupled laser systems in recent years. For systems of delay-coupled semiconductor lasers, achronal synchronization has been demonstrated experimentally [11] and studied theoretically [12]. For erbium doped fiber ring lasers (EDFRLs) chaotic behavior has been observed and modeled, demonstrating a rich variety of dynamical states [13–15]. Chaotic synchronization for coupled EDFRLs has also been observed and studied in depth [16, 17], and delay-coupled fiber ring lasers have also demonstrated properties of achronal synchronization and noise-induced synchronization [18].

Previous work has also considered noise-induced synchronization in EDFRLs connected via passive coupling delay lines. For two coupled lasers of this type, both modeling and experimentation have demonstrated a complex "leader-follower" phenomenon of dynamic achronal synchronization between the two lasers, where the offset of the phase is precisely equal to the

#152747 - $15.00 USD Received 11 Aug 2011; revised 21 Oct 2011; accepted 24 Oct 2011; published 15 Nov 2011
(C) 2011 OSA

delay time introduced by the passive coupling line [19–21]. In the case of the two coupled fiber ring lasers, the achronal synchronization is observed to be non-stationary in both theory and experiment, since leading and lagging lasers switch roles over the course of long time observations. Such behavior is an obstruction to long time synchronization in phase due to its random switching in an achronal state.

Our current work generalizes the EDFRL model for ring lasers to consider larger arrays than have been modeled previously. Specifically, we generate networks consisting of three or more ring lasers attached to one another through a central "hub" laser. In [22], it was shown for semiconductor laser networks modeled using the Lang-Kobayashi laser formulation [4], chaotic synchronization occurs in the star coupling formation if the number of lasers, N, is sufficiently large. Motivated by this result, we examined similar coupling arrangements for EDFRL lasers. In contrast to the chaotic semiconductor result, we show that there is very weak dependence on N. However, we observe a uniform scaling of synchronization onset as a function of weak coupling. The scaling appears to be independent of the number of lasers, N.

2. Mathematical model

Using the fiber ring model originally derived in [14], with modifications made in [23, 24] and [19], we consider an array of N ring lasers coupled via $N-1$ injection lines comprised of a passive single mode optical fiber, a splitter, and a variable attenuator. The model is characterized by the total population inversion, $W_i(t)$, of each ith laser (averaged over the length of the fiber amplifier) and the electric field $E_i(t)$ in each laser. Two delay times occur in the model: τ_R is the cavity round-trip time in the ring, and τ_d is the delay in the coupling between lasers. These delay terms correspond to the travel time of light in various components of the system, and thus resolve the spatial dependencies in the system normally modeled by the Maxwell-Bloch equations. The equations for the delay-coupled dynamics, including noise terms, are as follows:

$$E_j(t) = R\exp\left[\Gamma(1-i\alpha_j)W_j(t)+i\Delta\phi\right]E_j^{fdb}(t)+\xi_j(t) \tag{1}$$

$$\frac{dW_j}{dt} = q-1-W_j(t)-\left|E_j^{fdb}(t)\right|^2\left\{\exp\left[2\Gamma W_j(t)\right]-1\right\}, \tag{2}$$

where

$$E_j^{fdb}(t) = E_j(t-\tau_R)+\frac{1}{b_j}\sum_{k=1}^{N}B_{j,k}\kappa_k E_k(t-\tau_d). \tag{3}$$

$E_j(t)$ denotes the complex envelope of the electric field in laser j, measured at a given reference point inside of the cavity. E_j^{fdb} is the feedback for laser j and includes optical feedback within laser j and optical coupling with other lasers. Time is dimensionless, measured in units of the decay time of the atomic transition, $\gamma_{||}$. The active medium is characterized by the dimensionless detuning α_j between the transition and lasing frequencies, and by the dimensionless gain $\Gamma = \frac{1}{2}aL_aN_0$. Here a is the material gain, L_a the length of the active fiber, and N_0 the population inversion at transparency. Each ring cavity is characterized by its return coefficient R, which represents the fraction of light remaining in the cavity after one round-trip, and the average phase change $\Delta\phi = 2\pi nL_p/\lambda$ due to propagation of light with wavelength λ along the passive fiber of length L_p and index of refraction n. The energy input for each laser is given by the pump parameter q. The normalization term b_j is the number of lasers connected to laser j.

The coupling between lasers is through the field, and described by the connection matrix, B. Matrix B has components $B_{j,k} = 1$, if node j is directly connected to node k, and zero otherwise. For the star topology, B is symmetric since the coupling is assumed to be mutual, and given by

#152747 - $15.00 USD Received 11 Aug 2011; revised 21 Oct 2011; accepted 24 Oct 2011; published 15 Nov 2011
(C) 2011 OSA

the NxN matrix:

$$B = \begin{pmatrix} 0 & 1 & 1 & \dots & 1 \\ 1 & 0 & 0 & \dots & 0 \\ 1 & 0 & 0 & \dots & 0 \\ \vdots & \vdots & \vdots & \ddots & \vdots \\ 1 & 0 & 0 & \dots & 0 \end{pmatrix}. \tag{4}$$

By altering B in various ways, a variety of different connection schemes for coupled laser systems can be considered. The ξ_j terms model stimulated emission and are mean zero Gaussian noise applied to the system with standard deviation D. Coupling between the lasers is characterized by the coupling strength κ_j, the ratio of the power of light in the injection line to the power of light in the source ring, and only symmetric coupling is considered at the present time.

3. Numerical methods

The model system is simulated using an explicit time-discretization and integration scheme. Following the work of [19], the round-trip travel time τ_R is calculated from the length of the active and passive fibers,

$$\tau_R = (L_a + L_p) n \gamma_{||} / c, \tag{5}$$

where c is the the speed of light. For the purposes of discretization, the ring cavity is divided into N_s spatial elements, giving us a time discretization $\Delta t = \tau_R / N_s$.

For each time-step of integration, the new population inversion $W_j(t + \Delta t)$ is approximated using a second-order modified Euler method. New values of E_j and the feedback are computed directly from the formulas 1 and 3. The raw data is saved in a truncated time series from which the intensity $I_j = |E_j|^2$ is computed and then passed through a low-pass filter. For these simulations, a second order Butterworth filter from Matlab was used, and set with a threshold of 125 MHz, in keeping with experiments that use a bandwidth photo-detector set at that frequency [19, 24].

The results below are generated using random initial data for E_j, and initializing the inversion near a steady state. Simulations are run for a minimum of 3000–5000 round-trips in the ring so transients are removed. The parameter values used for all simulations listed in Table 1 are based on previous experimental and modeling efforts as reported in [19].

4. Results

We explore the synchronization properties of arrays of fiber lasers where the structure of the network is in a star configuration. The amplitude cross correlation of any two lasers labeled a and b over a time series of length K, is defined by

$$C_{ab} = \frac{1}{\sigma_a \sigma_b} \frac{1}{K} \sum_{j=1}^{K} \left[I_a(t_j - \tau_s) - \langle I_a \rangle \right] \left[I_b(t_j) - \langle I_b \rangle \right], \tag{6}$$

where τ_s is a time shift in the respective time series of the intensities $I_{a,b}$ of two lasers, and $\sigma_{a,b}$ are the standard deviations of the two time series. We expect the time series to be offset due to the delay in communication based on generalized synchronization analysis given in [25] for semiconductor lasers. Similarly, we define the phase coherence of two nodes as,

$$R_{ab} = \left| \frac{1}{K} \sum_{j=1}^{K} e^{\Delta \phi_{ab,j}} \right|, \tag{7}$$

where

$$\Delta \phi_{ab,j} = \phi_a(t_j - \tau_s) - \phi_b(t_j) \tag{8}$$

#152747 - $15.00 USD Received 11 Aug 2011; revised 21 Oct 2011; accepted 24 Oct 2011; published 15 Nov 2011
(C) 2011 OSA

Table 1. Summary of parameters used in the laser coupling model. The detuning parameter of the outer lasers was uniform, $\alpha_{out} = .0352$, while $\alpha_{in} = .0202$ was picked for the inner laser. For simplicity, the length of the fibers (and thus the delays) were fixed for all experiments, as were the coupling strengths.

Parameter	Value	Units	Description
R	0.4		output coupler return coefficient
a	2.03×10^{-23}	m^2	material gain coefficient
L_a	15	m	length of active fiber
L_p	27	m	length of passive fiber
N_0	10^{20}	m^{-3}	transparency inversion
Γ	0.0152		dimensionless gain
α_{in}	0.0202		detuning factor (inner laser)
α_{out}	0.0352		detuning factor (all outer lasers)
n	1.44		index of refraction
λ	1.55×10^{-6}	m	wavelength
$\Delta\phi$	1.58×10^{8}		average phase change
D	0.02		standard deviation of noise
q	40-200		pump parameter
$\gamma_{\|\|}$	100	s^{-1}	population decay rate
τ_R	201.6×10^{-9}	s	cavity round-trip time
τ_d	45×10^{-9}	s	delay time between lasers
κ	0-0.014		coupling strength

is the phase difference between the jth points of the intensities when Laser a leads Laser b. C ranges between -1 (negatively correlated) and 1 (perfectly correlated), while R ranges between 0 (no phase synchronization) and 1 (complete phase synchronization). Here the phase angle ϕ is defined as the arctangent of the ratio of the real and imaginary parts of the Hilbert transform of the intensity time series, following the convention found in [19].

It is inconvenient to write all the the various C_{ab} and R_{ab} terms for more than a few lasers, and so we introduce C_{out} and C_{in} as the mean value of the cross correlation of all outer lasers with one another, and all outer lasers with the inner hub, respectively. Analogous quantities are also defined on R. To measure synchronization lag between between the central laser and the outer lasers, we examine which values of time shift, τ_s, maximize the cross correlation C_{out} and C_{in}.

Figure 1 shows the mean cross correlation and phase coherence as a function of τ_s. The results were generated with coupling coefficient $\kappa = 0.009$ and a network of five lasers, four on the outside and one central hub. In this simulation the four outer lasers are detuned from the inner laser, with each laser having the identical detuning factor $\alpha_j = .0352$, while the detuning factor for the inner laser is $\alpha_j = .0202$. Note that when considering C_{in}, as in figure 1, with respect to τ_s we adopt the convention that the inner laser time series is the one being shifted backward, thus C_{in} here can be viewed as the cross correlation when the inner laser is leading. Note that in Figure 1, the outer lasers have an average peak cross and phase correlation at $\tau_s = 0$, meaning that the outer lasers synchronize with each other. Concurrently the outer lasers synchronize with the inner hub at $\tau_s = \tau_d$. This is consistent with the case of two connected fiber lasers, where the synchronization is offset by one factor of the delay time [11, 19, 25].

It is also worth noting that an additional local maximum of C_{out} and R_{out} occurs at $\tau_s = 2\tau_d$. This agrees with intuition, since the total time it takes for a signal from one outer laser to reach another is exactly two delay cycles. From repeated numerical experiments illustrating the

#152747 - $15.00 USD Received 11 Aug 2011; revised 21 Oct 2011; accepted 24 Oct 2011; published 15 Nov 2011
(C) 2011 OSA

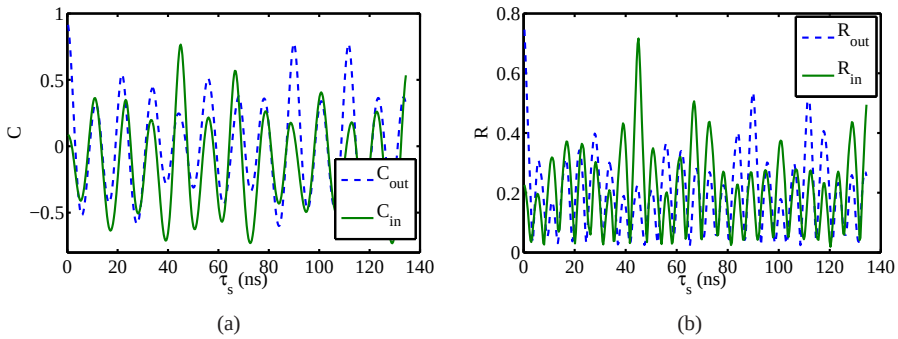

(a) (b)

Fig. 1. The cross correlation and phase coherence for $N = 5$ fiber ring lasers, as a function of a shift τ_s in the time series, for the star configuration. In this experiment, $\tau_d = 45$ns, and it is clear that C_{out} peaks at zero while C_{in} peaks at τ_d.

behavior described above, we can conclude that the outer lasers tend to synchronize with one another precisely, while the outer lasers tend to be offset by a factor of one delay with the inner laser.

Figure 2 illustrates the properties discussed above for a simulation of 5 lasers in the star formation. In this simulation, all 5 lasers are given random initial data, and the outer lasers are identically detuned from the inner laser. The central laser, in blue, is offset by τ_d, and its peaks line up with the outer lasers, all of which are synchronized.

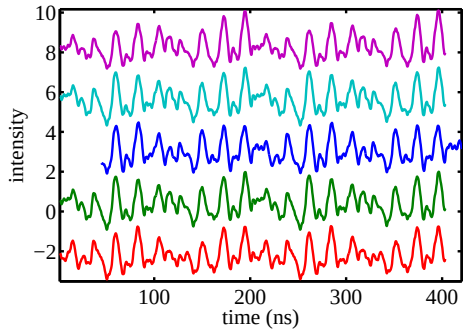

Fig. 2. A time history of the intensity for a numerical experiment with $N = 5$ and $\kappa = .01$. Here the inner "hub" laser (in blue) is shifted to the right by one delay because, in this experiment, the outer lasers are being led by the inner hub. Lasers 2–4 are shifted up or down by a small amount for illustrative purposes.

We next explore how adding additional outer lasers affects the overall synchronization of the system. Starting with $N = 3$, we run simulations with identical initial conditions and detuning parameters and examine the final state as a function of κ. Figure 3 shows how increasing the coupling strength causes the lasers to go from an unsynchronized to a synchronized state. Since the system (1-3) behaves like a two laser system when the outer lasers are synchronized, the initial conditions used in generating figure 3 are given by the final state of a two laser simulation (which is simulated long enough for transient effects to pass). In each experiment, all the outer lasers are given the same exact initial condition and prehistory as determined by one of the lasers in the two laser simulation, and the inner laser is given the prehistory associated with

#152747 - $15.00 USD Received 11 Aug 2011; revised 21 Oct 2011; accepted 24 Oct 2011; published 15 Nov 2011
(C) 2011 OSA

the other laser. The error bars shown are derived from doing batches of 20 runs with different random number seeds for the noise terms. Here, the values of C_{out} are taken with zero lag, and were computed over a time series of ten round-trips (τ_R). Note, as more lasers are added, the scaling behavior of the cross correlation does not change, but the run to run variance decreases, as evidenced by the smaller error bars on the cross-correlation of the outer lasers. We can conclude that adding lasers appears to diminish the variance due to noise, but does not enhance the overall synchronization scaling as a function of κ and N. Larger values of N were run (up to $N = 200$), with no noticeable improvement on the overall synchronization (for fixed κ), though these are not shown in Figure 3.

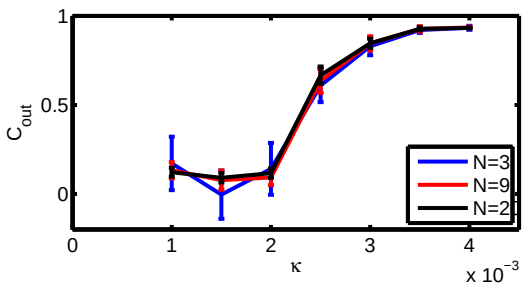

Fig. 3. Here we demonstrate the growth of the cross-correlation for $N = 3$, $N = 9$ and $N = 20$ lasers as a function of κ. Here C_{out} is recorded with $\tau_s = 0$ over ten cavity round trips. Note that the smallest values of κ represent a nearly uncoupled system.

Simulations were also run for randomly distributed detuning parameters for the outer lasers for comparison with crowd synchrony results obtained in [26]. However, enhanced synchronization was not observed for large numbers of lasers in this regime. Although several factors could be attributed to the difference in results, it should be noted that the lasers modeled here exhibit noise-induced oscillations, while those in [26] exhibit chaotic oscillations. These observations will be explored in-depth in a coming article.

5. Weak pumping limit

As a variation, we follow the work in [27] that in the star coupling configuration, outer lasers tend to synchronize, even if the pump rate of the inner laser is very low. In fact, in certain configurations, the "weak link synchronization" actually enhances synchronization properties when the oscillators are chaotic. Although the coupling considered in [27] is different than what is considered here, their coupling is evanescent and nearest neighbor, while we focus on injection line intensity coupling, we would like to see if some of these effects persist in our model. In Figure 4, we turn the pump constant q to be 40 for the center laser, while $q = 200$ for all outer lasers, and observe that the lasers still synchronize for small values of κ. In this regime, the outer lasers synchronize with one another, even though the amplitudes of the outer and inner laser(s) are not correlated.

6. Conclusion

We considered a star coupling configuration of N coupled fiber ring lasers in the weak coupling limit. The model we considered replaced the spatial component of the ring laser with a time delay. In addition, delay was included in coupling fibers used for communication. Using this model, we have shown synchronization in both amplitude and phase of the measured intensities can occur by measuring the cross correlation between inner hub and outer lasers. When

#152747 - $15.00 USD Received 11 Aug 2011; revised 21 Oct 2011; accepted 24 Oct 2011; published 15 Nov 2011
(C) 2011 OSA

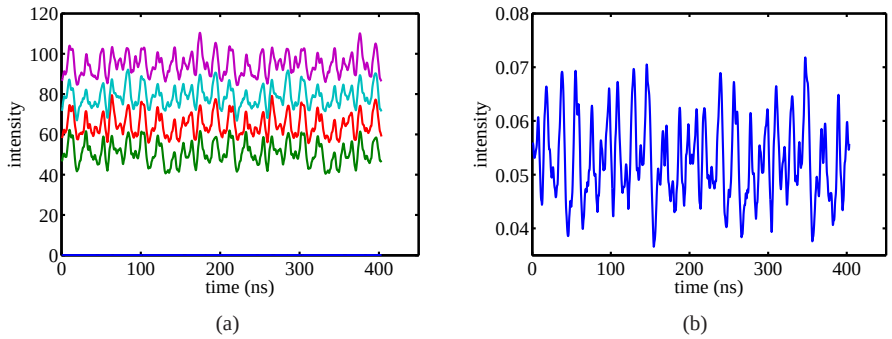

Fig. 4. Achronal synchronization for the weak pumping case. Here the outer lasers have $q = 200$ while the inner have $q = 40$. Here $\kappa = .01$. The inner laser here is in blue and is blown up in Figure 4b. Here $C_{out} \sim .901$.

examining cross correlation between outer lasers only, we find that synchronization occurs with zero-lag. This is consistent with the results reported in [27], where the outer lasers of evanescently coupled fibers synchronize in the absence of delay. In contrast with the outer lasers, the cross correlation between the hub and outer lasers exhibits lag synchrony with the lag time equal to the coupling delay between lasers. That is, as a group, the outer leaders lead or lag the hub with approximately the same waveform on average.

In the weak pumping limit as the pump of hub approaches threshold, we observe similar results. As a function of the number of lasers, N, we do not see a threshold for synchronization onset, however, the type of coupling considered here is different from that studied in Lang-Kobayashi laser models in [26], so perhaps this result is to be expected. Physically, we understand the onset of synchronization by equating the array to a mutually delay coupled system of three lasers, as reported and analyzed in [25]. In that work the end lasers synchronize while they appear uncorrelated with the inner, or hub, laser. The idea is that the hub laser is in generalized synchronization with the outer lasers, through a nonlinear function which is unknown [28]. By analyzing the dynamics transverse to the synchronization sub-manifold containing the end lasers, sufficient conditions for stability may be derived in the case of semiconductor lasers.

On the other hand, in systems of two delay coupled lasers, lag synchronization is also observed. By averaging over the temporal dynamics of the outer lasers in our ring laser system, the system may be considered to similar to a two-laser delay coupled system, where lag synchronization is understood. That is, the cross correlation between the two lasers peaks not at zero, but at lag time equal to the delay. This has also been observed in two laser systems [19, 21]. The theoretical analysis of this will be presented elsewhere for the fiber ring lasers in the hub formation.

Acknowledgments

This work is supported by the Office of Naval Research. Brandon Lindley is currently an NRC Postdoctoral Fellow. The authors would like to acknowledge Leah Shaw for providing original source code that was useful in obtaining these results. The authors would also like to acknowledge Rajarshi Roy for providing insightful comments after reading a late draft of this paper.